

1 Routine monitoring of Western Lake Erie to track water quality
2 changes associated with cyanobacterial harmful algal blooms

3
4 Anna G Boegehold¹, Ashley M. Burtner¹, Andrew C Camilleri¹, Glenn Carter¹, Paul DenUyl¹,
5 David Fanslow², Deanna Fyffe Semenyuk^{1,3}, Casey M Godwin¹, Duane Gossiaux², Thomas H
6 Johengen¹, Holly Kelchner¹, Christine Kitchens¹, Lacey A. Mason², Kelly McCabe¹, Danna
7 Palladino², Dack Stuart^{1,4}, Henry Vanderploeg², Reagan Errera²

8
9
10 ¹Cooperative Institute for Great Lakes Research (CIGLR), University of Michigan, 4840 South
11 State Road, Ann Arbor, MI 48108, USA

12 ²NOAA Great Lakes Environmental Research Laboratory, 4840 South State Road, Ann Arbor,
13 MI 48108, USA

14 ³Jacobs, 1999 Bryan Street, Suite 1200, Dallas, TX, 75201, USA

15 ⁴Woods Hole Group, Inc., 107 Waterhouse Road, Bourne, MA 02532

16
17 *Correspondence to:* Anna G Boegehold (annaboeg@umich.edu) & Reagan Errera
18 (reagan.errera@noaa.gov)

19 **Abstract**

20 The western basin of Lake Erie has a history of recurrent cyanobacterial harmful algal blooms
21 (HABs) despite decades of efforts by the United States and Canada to limit phosphorus loading,
22 a major driver of the blooms. In response, the National Oceanic and Atmospheric Administration
23 (NOAA) Great Lakes Environmental Research Laboratory (GLERL) and the Cooperative
24 Institute for Great Lakes Research (CIGLR) created an annual sampling program to detect,
25 monitor, assess, and predict HABs in western Lake Erie. Here we describe the data collected
26 from this monitoring program from 2012 to 2021. This dataset includes observations on physico-
27 chemical properties, major nutrient fractions, phytoplankton pigments, microcystins, and optical
28 properties for western Lake Erie. This dataset is particularly relevant for creating models,
29 verifying and calibrating remote sensing algorithms, and informing experimental research to
30 further understand the water quality dynamics that influence HABs in this internationally
31 significant body of freshwater. The dataset can be freely accessed from NOAA National Centers
32 for Environmental Information (NCEI) at <https://doi.org/10.25921/11da-3x54> (Cooperative
33 Institute for Great Lakes Research, University of Michigan; NOAA Great Lakes Environmental
34 Research Laboratory, 2019).

Deleted: nutrient

Deleted: enable

37 Introduction

38 Lake Erie is situated on the international boundary between the United States and
39 Canada and is the smallest by volume of the five Laurentian Great Lakes. It is ecologically,
40 culturally, and economically significant to the approximately 12.5 million people who live in the
41 watershed. Each year Lake Erie supports nearly 14,000 tonnes of commercial and traditional
42 fisheries, over 33,000,000 tonnes of freight, and over \$1.5 million in recreation and tourism
43 business (Sternner et al., 2020). Lake Erie has endured multiple anthropogenic stressors since
44 European settlement in the area, most notably the draining of coastal wetlands for development
45 of agricultural lands in the late 18th century (Allinger and Reavie, 2013). Currently, the
46 ecological state of Lake Erie is considered poor, partially due to excess nutrient input that
47 supports harmful algal blooms (HABs; ECCC and US EPA, 2022). These seasonal HABs are
48 typically dominated by toxin producing cyanobacteria, causing concern for public and
49 ecosystem health (Watson et al., 2016). Humans can be exposed to cyanotoxins through
50 ingestion of contaminated fish and drinking water and through inhalation and dermal exposure
51 during recreational events such as swimming and boating (Carmichael and Boyer, 2016; Buratti
52 et al., 2017). Cyanotoxins can also cause illness and death in aquatic and terrestrial animals
53 (Carmichael and Boyer, 2016). The economic cost of HABs impacts in Lake Erie is estimated to
54 be hundreds of millions of dollars each year (Smith et al., 2019).

55 To combat the deteriorated state of Lake Erie water quality, bi-national water resource
56 management policies alongside scientific research and water quality monitoring efforts have
57 been underway for decades. The Great Lakes Water Quality Agreement (GLWQA), first signed
58 in 1972, was a commitment between the US and Canada in response to degraded water quality
59 throughout the Great Lakes ecosystem (GLWQA, 2012). Phosphorus was found to be the key
60 nutrient that was promoting excess phytoplankton growth (Charlton et al., 1993), and thus the
61 GLWQA sought to limit total phosphorus input to the lakes in an attempt to reduce

62 phytoplankton growth and biomass (Steffen et al., 2014). The 1972 Clean Water Act (CWA) was
63 similarly enacted to regulate [point-source](#) pollution discharge, including phosphorus, into
64 navigable waters in the United States. After the signing and implementation of the phosphorus
65 load reduction practices outlined in the GLWQA and CWA, the water quality of Lake Erie
66 improved and the lake experienced a period of restoration (Makarewicz and Bertram, 1991).
67 This success was attributed to upgrades to sewage treatment plants and industrial discharges
68 which reduced phosphorus loading from point sources by 50% within ten years of peak levels
69 observed in 1968 (Charlton et al., 1993; Joosse and Baker, 2011; Steffen et al., 2014).

70 While the water quality of Lake Erie rebounded in the 1980s and early 1990s, by the mid
71 1990s and early 2000s annual HAB events were occurring in Lake Erie again, particularly in the
72 warm, shallow western basin (Allinger and Reavie, 2013; Kane et al., 2015; Watson et al.,
73 2016). Total phosphorus loading has been relatively stable in Lake Erie from the 1980s onward
74 (Dolan and Chapra, 2012; Watson et al., 2016), and although [point-source](#) phosphorus loading
75 controls had been a successful mitigation measure at one point, several anthropogenic
76 stressors within the watershed were exacerbating the issue of poor water quality. An increase in
77 agricultural sources of biologically available soluble nutrients, legacy phosphorus in the Lake
78 Erie watershed, altered nutrient cycling by invasive dreissenid mussels, and climate change are
79 thought to be primarily responsible for the HABs resurgence (Vanderploeg et al., 2001; Conroy
80 et al., 2005; Bridoux et al., 2010; Michalak et al., 2013; Matisoff et al., 2016; Huisman et al.,
81 2018; Van Meter et al., 2021).

82 The post-recovery period HABs have predominantly been composed of the
83 cyanobacteria species *Microcystis aeruginosa* along with genera *Anabaena*, *Aphanizomenon*,
84 *Dolichospermum*, and *Planktothrix* (Steffen et al., 2014; Watson et al., 2016). These
85 cyanobacteria can produce an array of several types of phycotoxins, with the most common
86 being a suite of hepatotoxins known as microcystins (MCs). Microcystins primarily affect the
87 liver but can also cause adverse health effects on the kidneys, brain, and reproductive organs

88 (Carmichael and Boyer, 2016). Phycotoxins are commonly present during Lake Erie HABs, and
89 in August 2014 the city of Toledo, OH drinking water supply was contaminated with MCs,
90 leaving >400,000 without clean drinking water (Steffen et al., 2017).

91 To understand HAB events in US waterways, Congress authorized the Harmful Algal
92 Bloom and Hypoxia Research and Control Act in 1998 (HABHRCA; Public Law 115-423) which
93 mandated the National Oceanic and Atmospheric Administration (NOAA) to “advance the
94 scientific understanding and ability to detect, monitor, assess, and predict HAB and hypoxia
95 events”. Under HABHRCA, the NOAA Great Lakes Environmental Research Lab (GLERL),
96 NOAA National Centers for Coastal Ocean Science (NCCOS), and the Cooperative Institute for
97 Great Lakes Research (CIGLR; formerly CILER - Cooperative Institute for Limnology and
98 Ecosystems Research) developed an ecological forecast to predict HAB events in Lake Erie.
99 Starting in 2008, researchers at these institutes began using remote sensing to monitor
100 seasonal HABs, created a seasonal forecast system based on spring P loads, and developed
101 models to predict short-term bloom changes to alert stakeholders and the public (Rowe et al.,
102 2016). Products from these efforts, known as Lake Erie Harmful Algal Bloom Forecasts, are
103 freely available during the bloom season at [https://coastalscience.noaa.gov/research/stressor-](https://coastalscience.noaa.gov/research/stressor-impacts-mitigation/hab-forecasts/lake-erie/)
104 [impacts-mitigation/hab-forecasts/lake-erie/](https://coastalscience.noaa.gov/research/stressor-impacts-mitigation/hab-forecasts/lake-erie/).

105 *In-situ* sampling of the bloom was necessary to calibrate and validate the remote
106 sensing images and models as well as measure microcystin concentration. Sampling events
107 were led by personnel at GLERL and CIGLR starting in 2008 and were designed to collect
108 discrete samples within the extent of the bloom area. At first, samples were taken
109 opportunistically within the bloom and sampling locations and analytical parameters were
110 inconsistent. In 2009, regular sampling stations were identified based on spatial patterns of the
111 bloom. From 2009 to 2011, in addition to opportunistic samples, nine main stations in the
112 western basin of Lake Erie were sampled intermittently from June through October (Bertani et
113 al., 2017; Rowland et al., 2020). While these sampling efforts initially began to complement

114 existing research products, the experimental nature of the 2008 to 2011 sampling cruises also
115 provided insight into creating a regular monitoring program that would support critical research
116 and product development related to western Lake Erie HABs.

117 In 2012, researchers at GLERL and CIGLR, with support from the Great Lakes
118 Restoration Initiative (GLRI), formalized a sampling regimen to monitor the spatial and temporal
119 variability of seasonal HAB events in western Lake Erie (WLE). The establishment of this
120 monitoring program corresponded with increased federal emphasis on evaluating trends and
121 drivers of WLE HABs and water quality. Four monitoring stations were identified and regular
122 surface samples were collected from May to September and analyzed for nutrient, pigment, and
123 particulate microcystin concentrations (Figs. 1 & 2). In following years, the monitoring program
124 evolved and expanded. New stations were added to better characterize the bloom and
125 complement other observing systems. Sampling parameters were adjusted and added based on
126 the needs of current research (Table 1). Results of these sampling cruises were compiled and
127 distributed informally upon request until 2019 when the data were organized and archived on
128 the NOAA National Centers for Environmental Information (NCEI) open-access data repository
129 (<https://www.ncei.noaa.gov/>).

130 Long term monitoring of WLE is fundamental to the continual assessment of water
131 quality changes in response to both stressors and water quality management efforts (Hartig et
132 al., 2009, 2021). The GLERL/CIGLR monitoring data has been used by numerous researchers
133 to develop and assess models (Rowe et al., 2016; Weiskerger et al., 2018; Fang et al., 2019;
134 Liu et al., 2020; Qian et al., 2021; Wang and Boegman, 2021; Hellweger et al., 2022; Maguire et
135 al., 2022), to calibrate remote sensing algorithms (Sayers et al., 2016, 2019; Avouris and Ortiz,
136 2019; Bosse et al., 2019; Vander Woude et al., 2019; Pirasteh et al., 2020; Xu et al., 2022), and
137 to elucidate ecological mechanisms and complement experimental data (Cory et al., 2016;
138 Reavie et al., 2016; Berry et al., 2017; Steffen et al., 2017; Kharbush et al., 2019, 2023; Newell

139 et al., 2019; Den Uyl et al., 2021; Smith et al., 2021, 2022; Hoffman et al., 2022; Marino et al.,
140 2022; Yancey et al., 2022a, b).

141 The objective of this paper is to inform users of the dataset “Physical, chemical, and
142 biological water quality monitoring data to support detection of Harmful Algal Blooms (HABs) in
143 western Lake Erie, collected by the Great Lakes Environmental Research Laboratory and the
144 Cooperative Institute for Great Lakes Research since 2012” by describing the data generated
145 from this monitoring program and detailing how samples were collected and analyzed. This
146 paper contextualizes this long-term data set so that it can continue to be used to benefit our
147 collective ecological knowledge of western Lake Erie.

148

149 Table 1. Description of stations sampled in western Lake Erie from 2012 to 2021. Latitude and
150 longitude (decimal degree) coordinates for each station are target locations as the boat was
151 allowed to drift at each site during *in-situ* sampling.

152

Station	Latitude	Longitude	Avg. Depth (m)	Years Monitored
WE02	41.762	-83.330	5.4	2012-2021
WE04	41.827	-83.193	8.4	2012-2021
WE06	41.705	-83.385	2.9	2012-2021
WE08	41.834	-83.364	4.8	2012-2021
WE09	41.718	-83.424	2.7	2016-2021
WE12	41.703	-83.254	6.6	2014-2021
WE13	41.741	-83.136	8.9	2014-2021
WE14	41.720	-83.010	9.3	2015
WE15	41.617	-83.009	4.5	2015-2017
WE16	41.660	-83.143	6.2	2018-2021

153

154 Methods

155 Study Site

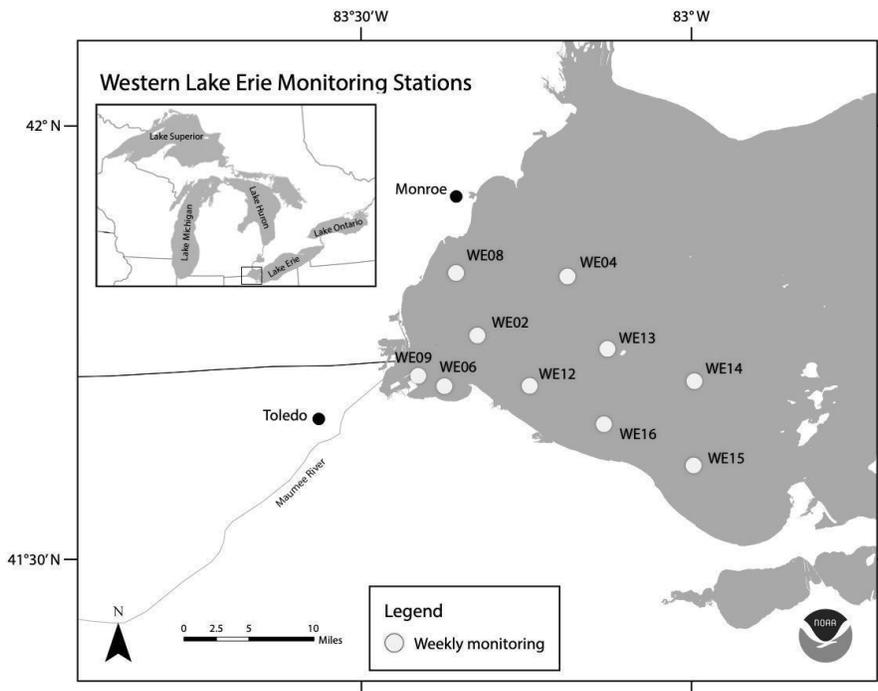
156 Based on the lake's bathymetry, Lake Erie can be divided into the eastern, central, and
157 western basins which in turn influence physical and biological processes (Allinger and Reavie,
158 2013). The data presented in this paper were collected from the western basin, which
159 encompasses the western part of the lake to Point Pelee, ON, Canada and Cedar Point, OH,
160 USA (Fig. 1). The well-mixed western basin is the shallowest (maximum average depth of 11
161 m), warmest, and most productive of the three basins. Although it's typical for temperate WLE to
162 have ice cover in the winter (Jan to Mar), summer (Jul to Sep) surface water temperatures often
163 reach or exceed 25 °C. The western basin receives 95% of its hydraulic inflow from the Detroit
164 River, which connects Lake Erie hydrologically to Lake Huron via the St. Clair River and Lake
165 St. Clair (Cousino et al., 2015). Among the other tributaries to WLE (including River Raisin,
166 Portage River, Ottawa River, Stony Creek, Swan Creek, and Sandusky River), the Maumee
167 River discharges into the western basin near the city of Toledo, Ohio and contributes a
168 significant amount of sediments and nutrients to the entire Lake Erie basin (Baker et al., 2014a,
169 [b; Rowland et al. 2020; see NCWQR 2022 for Maumee River water quality data](#)). Nutrient and
170 sediment loads from the Maumee River can vary with precipitation, where stormwater runoff can
171 provide a pulse of nutrients into the basin, potentially altering cyanobacteria dynamics (Baker et
172 al., 2014a; King et al., 2022). Land use in the Lake Erie watershed is 75% agricultural and 11%
173 urban, both of which contribute to the large amounts of soluble reactive phosphorus into the
174 basin (Mohamed et al., 2019; Myers et al., 2000).

175 This dataset includes water quality data from ten monitoring stations on the United
176 States side of WLE that were sampled from 2012 to 2021 (Figs. 1 & 2, Tables 1 & 2). The

177 average depth of monitoring stations ranged from 2.7 m at WE9 to 9.3 m at WE14. These sites
178 were chosen to reflect the various nutrient and hydrologic inputs and gradients into WLE, as
179 well as represent areas of the basin that are prone to HABs. The Maumee River inflow was a
180 major consideration in determining these sites. The initial 4 stations sampled in this program
181 (WE02, WE04, WE06, and WE08) were selected because they were consistently within the
182 WLE blooms occurring at the time. Additional sites were later added to better represent the
183 spatial extent of HABs and to augment existing data provided by moored buoy continuous
184 monitoring systems, advanced monitoring technologies, such as Environmental Sample
185 Processors (Den Uyl et al., 2022), and other monitoring programs in WLE.

186 Field Sampling

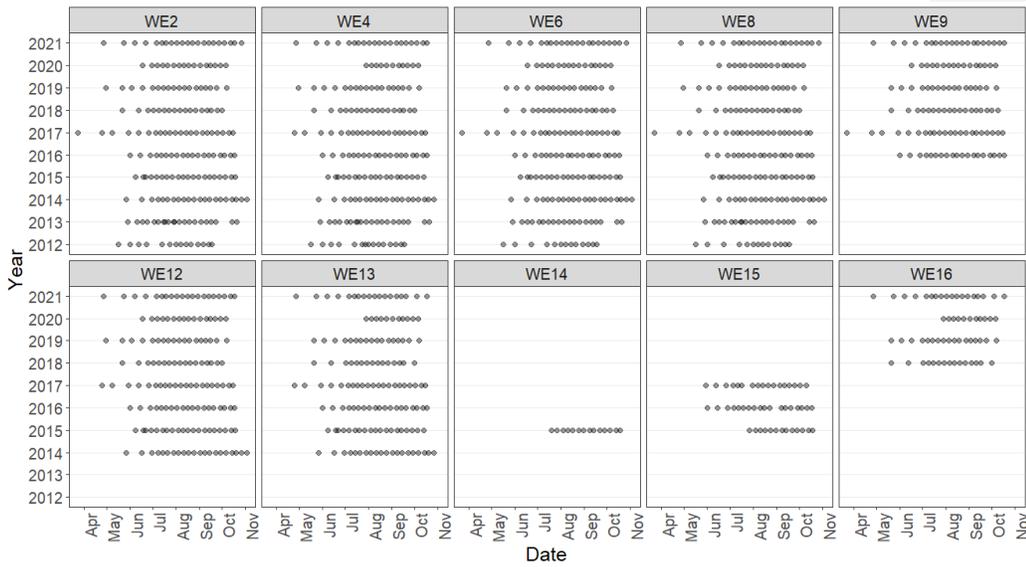
187 Western Lake Erie discrete field sampling was accomplished using NOAA GLERL
188 research vessels. Sampling took place during ice-free months and aimed to quantify the
189 environmental conditions prior to, during, and at the end of the bloom (Fig. 2). Sampling stations
190 represent approximate locations (Table 1; Fig. 1); *in situ* measurements and sampling were
191 collected once the boat reached the targeted location and then proceeded to drift during
192 sampling. The frequency and timing of those cruises varied over the first few years but has been
193 consistent since 2017 (Fig. 2). Sampling was disrupted in 2020 due to the global COVID-19
194 pandemic and resulting public health restrictions. In 2020, sampling was initiated in mid-June at
195 a reduced number of sites for select water quality parameters. In July, sampling stations and
196 parameters were expanded and all stations and parameters were sampled and measured by
197 August 2020. The prior standard sampling schedule resumed in April 2021.



198

199 Figure 1. Location of western Lake Erie water quality monitoring stations. This map was

200 provided by NOAA for use in this publication.



201
 202 Figure 2. Sampling frequency for each monitoring station for years sampled between 2012 to
 203 2021.

204
 205 *In-situ* measurements for conductivity, temperature, dissolved oxygen (DO), beam
 206 attenuation, transmission, and photosynthetically active radiation (PAR) were taken with a Sea-
 207 Bird 19plus V2 conductivity, temperature, and depth (CTD) profiler attached to a hydraulic
 208 crane. Data were collected on the downcast and were reported as the mean of recorded values
 209 within ± 0.5 m of the discrete sample depth. In 2012, sample temperature was taken on the boat
 210 with a Vee Gee Scientific IP67-rated digital thermometer. Sky conditions were recorded at the
 211 discretion of the field technician at each station during the sampling cruise. A Secchi disk was
 212 lowered into the water on the shaded side of the boat at each station and the depth at which the
 213 Secchi disk was no longer visible was recorded (Wetzel and Likens, 2000).

214 Water column samples were collected using a 5 L vertical Niskin bottle (General
 215 Oceanics model 1010). Niskin casts were evenly distributed between one or more high-density

216 polyethylene bottles that were rinsed with site water and stored in a cooler. Three to four Niskin
217 casts were used to fill the bottles, such that each bottle is a composite sample of the water
218 collected. Surface samples were taken 0.75 m below the water's surface, mid-column samples
219 were taken at approximately 4.25 m below surface, and benthic or bottom samples were taken
220 at approximately 0.5 m above the lake bottom at each station. Surface samples were taken at
221 all stations while mid-column and benthic sample collection varied between sites and years.
222 Scum samples of dense cyanobacterial accumulation on the surface of the water were collected
223 opportunistically using a 2 L modified Van Dorn water sampler. Sampling times were reported
224 as Eastern Daylight Time (UT -4:00). Upon arrival at the laboratory, raw water samples were
225 immediately subsampled and preserved until analysis.

226 Wind speed and wave height data were obtained from moored buoy continuous
227 monitoring systems in proximity to sampling stations for a timestamp that corresponded to the
228 time samples were collected at that station. Wave height data for all stations were obtained from
229 the Toledo Intake Buoy (owned and maintained by Limnotech Inc.). Wind speed data for
230 stations WE02, WE06, WE09, WE12, WE14, WE15, and WE16 were also collected from this
231 buoy. Data for this buoy is available through the Great Lakes Observing System (GLOS;
232 platform ID 45165, <https://seagull.glos.org/data-console/71>). Wind speed data for stations
233 WE04, WE08, and WE13 were obtained from the Toledo Harbor Light no. 2 buoy (Station
234 THLO1, owned and maintained by GLERL). Data for this buoy is available through NOAA's
235 National Data Buoy Center (https://www.ndbc.noaa.gov/station_realtime.php?station=THLO1).
236

237 Laboratory analysis of samples

238 Water collected from WLE was subsampled to make a range of analytical
239 measurements in the laboratory (Table 2).

240

241 Table 2. Summary of parameters reported in the dataset. [Wind speed and wave height data are](#)
242 [collected from moored buoy continuous monitoring systems which provide the data in Imperial](#)
243 [units.](#)

Parameter	Years monitored	Method
Surface samples (n=1296)	2012-2021	n/a
Mid-column samples (n=19)	2015	n/a
Benthic samples (n=512)	2015-2021	n/a
Station depth (m)	2012-2021	Sea-Bird 19plus V2 CTD profiler
Time of sampling (Eastern Daylight Time UTC -4:00)	2012-2021	n/a
Latitude (decimal degree)	2012-2021	n/a
Longitude (decimal degree)	2012-2021	n/a
Wind speed (knots)	2015-2021	Moored buoy continuous monitoring systems
Wave height (ft)	2012-2021	Moored buoy continuous monitoring systems
Cloud cover (sky)	2012-2021	Qualitative description
Secchi depth (m)	2012-2021	Wetzel and Likens (2000)
Sample temperature (°C)	2012	Vee Gee Scientific digital thermometer
CTD temperature (°C)	2013-2021	Sea-Bird 19plus V2 CTD profiler
CTD specific conductivity ($\mu\text{S cm}^{-1}$)	2013-2021	Sea-Bird 19plus V2 CTD profiler
CTD beam attenuation (m^{-1})	2013-2021	Sea-Bird 19plus V2 CTD profiler
CTD transmission (%)	2013-2021	Sea-Bird 19plus V2 CTD profiler
CTD dissolved oxygen (DO; mg L^{-1})	2013-2021	Sea-Bird 19plus V2 CTD profiler
CTD photosynthetically active radiation (PAR; $\mu\text{E m}^{-2} \text{s}^{-1}$)	2013-2021	Sea-Bird 19plus V2 CTD profiler

Deleted: n/a

Turbidity (NTU)	2013-2021	EPA Method 180.1
Particulate microcystins ($\mu\text{g L}^{-1}$)	2012-2021	Wilson et al. (2008)
Dissolved microcystins ($\mu\text{g L}^{-1}$)	2014-2021	Wilson et al. (2008)
Phycocyanin ($\mu\text{g L}^{-1}$)	2012-2021	Horvath et al. (2013)
Chlorophyll a ($\mu\text{g L}^{-1}$)	2012-2021	Speziale et al. (1984)
Total phosphorus (TP; $\mu\text{g L}^{-1}$)	2012-2021	Standard Method 4500-P
Total dissolved phosphorus (TDP; $\mu\text{g L}^{-1}$)	2012-2021	Standard Method 4500-P
Soluble reactive phosphorus (SRP; $\mu\text{g L}^{-1}$)	2012-2021	Standard Method 4500-P
Ammonium-N ($\mu\text{g L}^{-1}$)	2012-2021	Standard Method 4500-nh3-nitrogen (Ammonium)
Nitrate-N + Nitrite-N (mg L^{-1})	2012-2021	Standard Method 4500-no3-nitrogen (nitrate)
Urea-N ($\mu\text{g L}^{-1}$)	2016-2017	Milvenna and Savidge (1992), Goeyens et al. (1998), Chaffin and Bridgeman (2014)
Particulate organic carbon (POC; mg L^{-1})	2012-2021	Hedges and Stern (1984)
Particulate organic nitrogen (PON; mg L^{-1})	2012-2021	Hedges and Stern (1984)
Colored dissolved organic material (CDOM; m^{-1})	2014-2021	Binding et al. (2008), Mitchell et al. (2003)
Dissolved organic carbon (DOC; mg L^{-1})	2012-2017	APHA Standard Method 5310 B
Total suspended solids (TSS; mg L^{-1})	2012-2021	APHA Standard Method 2540
Volatile suspended solids (VSS; mg L^{-1})	2012-2021	APHA Standard Method 2540

Deleted: Ammonia

Deleted: ammonia

245

246 Optical properties

247 Turbidity was measured on raw samples using a Hach 2100AN Turbidimeter following
 248 US EPA method 180.1 (1993). Colored dissolved organic material (CDOM, also defined as
 249 chromophoric dissolved organic matter) was determined by filtering lake water through an acid

252 rinsed 0.2 µm nuclepore polycarbonate filter into acid-washed and combusted borosilicate vials.
253 Optical density of the filtered samples was then measured using a Perkin Elmer UV/VIS
254 Lambda 35 spectrophotometer at wavelengths from 300-800 nm. CDOM absorption was
255 calculated at 400 nm (Mitchell et al., 2003; Binding et al., 2008).

256 Dissolved organic carbon (DOC) concentrations were determined following American
257 Public Health Association (APHA) Standard Method 5310 B. Briefly, lake water was filtered
258 through 0.45 µm polyvinylidene difluoride membrane filters into combusted borosilicate glass
259 vials and frozen at -20°C until analysis. The filtrate was acidified with HCl and sparged with air
260 for 6 min before being analyzed on a Shimadzu total organic carbon analyzer.

261 Duplicate samples for particulate organic carbon (POC) and particulate organic nitrogen
262 (PON) were collected onto pre-combusted glass fiber filters and analyzed following Hedges and
263 Stern (1984) Samples were stored at -20 °C until analysis. The filters were then acidified by
264 fumigation with 10% HCl and dried at 70°C for 24 h before being quantified on a Perkin Elmer
265 2400 or a Carlo-Erba 1110 CHN elemental analyzer.

266 Total suspended solids (TSS) and volatile suspended solids (VSS) were determined via
267 gravimetric analysis following APHA Standard Method 2540. A known volume of lake water was
268 filtered through a pre-combusted, pre-weighed Whatman GF/F glass fiber filter. The filters were
269 then dried at 60° C for at least 24 h and reweighed. The difference in mass between the pre-
270 weighed and processed filter was reported as TSS. Volatile suspended solids concentrations
271 were quantified by combusting the filters used for TSS analysis at 450 °C for 4 h, weighing the
272 combusted filters, and calculating the mass lost.

273 Nutrient fractions

274 Total phosphorus (TP) and total dissolved phosphorus (TDP) samples were collected in
275 duplicate by subsampling 50 mL (2012 to 2019) or 20 mL (2020 to 2021) of lake water into acid
276 washed glass tubes and by filtering 20 mL of lake water through a 0.2 µm membrane filter and

277 collecting the filtrate, respectively. Samples for TP and TDP were refrigerated until samples
278 were digested with potassium persulfate solution and autoclaved at 121°C for 30 min, modified
279 from APHA Standard Method 4500-P. Digested TP and TDP samples were stored at room
280 temperature until concentrations were measured on a Seal QuAAtro continuous segmented flow
281 analyzer (SEAL Analytical Inc.) from 2012 to 2019 and a Seal AA3 from 2020 to 2021 using the
282 ascorbic acid molybdenum method as detailed by the instrument manual and APHA Standard
283 Method 4500-P. Analytical detection limits for the analyses were taken from the instrument
284 manufacturer's documentation.

285 Soluble reactive phosphorus (SRP), ammonium, nitrate + nitrite, and urea were each
286 determined by filtering 12 mL of lake water through a 0.2 µm membrane filter into 15 mL
287 centrifuge tubes during field sampling. Sample filtrates were stored at -20 °C upon receipt at the
288 laboratory. Soluble reactive phosphorus, ammonium, and nitrate + nitrite concentrations were
289 determined simultaneously on a Seal AA3 continuous segmented flow analyzer. Soluble
290 reactive phosphorus concentrations, like TP and TDP concentrations, were measured using the
291 ascorbic acid molybdenum method as detailed by the instrument manual and APHA Standard
292 Method 4500-P. Ammonium concentrations were measured using Bertholet reactions according
293 to the instrument manual and APHA Standard Method 4500-nh3-nitrogen. Nitrate + nitrite
294 concentrations were measured using copper-cadmium reduction methods according to the
295 instrument manual and APHA Standard Method 4500-no3-nitrogen. Analytical detection limits
296 for these inorganic nutrient analyses were taken from the instrument manufacturer's
297 documentation. Urea samples were measured by adding diacetyl monoxime and
298 thiosemicarbazide to the filtrate and briefly vortexing to mix, followed by adding sulfuric acid and
299 ferric chloride to the solution and briefly vortexing to mix. Samples were then incubated in the
300 dark for 72 h at room temperature before absorbance at 520 nm was read on a Perkin Elmer
301 UV/VIS Lambda 35 spectrophotometer. Urea concentrations were then quantified using a
302 standard curve (Mulvenna and Savidge, 1992; Goeyens et al., 1998; Chaffin and Bridgeman,

Deleted: ammonia

Deleted: ammonia

Deleted: Ammonia

306 2014). The detection limit was calculated using the standard deviation of repeated
307 measurements.

308 Photopigments and microcystins

Deleted: Pigments

309 Particulate phycocyanin and chlorophyll *a* concentrations were determined by filtering a
310 known volume of lake water under low vacuum (<200 mm Hg) onto 47 mm Whatman GF/F
311 glass fiber filters (Cytiva Life Sciences). Particulate phycocyanin sample filters were stored in 15
312 mL conical polypropylene centrifuge tubes and chlorophyll *a* sample filters were stored in amber
313 glass vials at -20 °C until analysis. Analysis methods for particulate phycocyanin were derived
314 from Horváth et al. (2013) where 9 mL of phosphate buffer was added to sample tubes and samples
315 were agitated using a shaker at 5 °C for 15 min at 100 rpm then vortexed for 10 s each. To
316 encourage cell lysis, samples were subjected to three freeze/thaw cycles at -20 °C followed by
317 sonication for 20 min using a Fisher FS110 H sonicator. Fluorescence of the extracted samples was
318 measured using an Aquafluor 8000-010 fluorometer (Turner Designs) with excitation from 400-600
319 nm and emission filter of >595 nm. Particulate phycocyanin was calibrated annually against C-
320 Phycocyanin material from Sigma-Aldrich. Analysis methods for chlorophyll *a* were derived from
321 Speziale et al. (1984) where chlorophyll *a* was extracted from samples using dimethylformamide
322 and placed into a 65 °C water bath for 15 min. Samples were then cooled to room temperature
323 and vortexed for 15-20 s before being quantified using a 10 AU fluorometer (Turner Designs)
324 with excitation filter of 436 nm and emission at 680 nm. Phycocyanin and chlorophyll *a*
325 procedures were performed under low or green light to reduce pigment degradation within the cell.

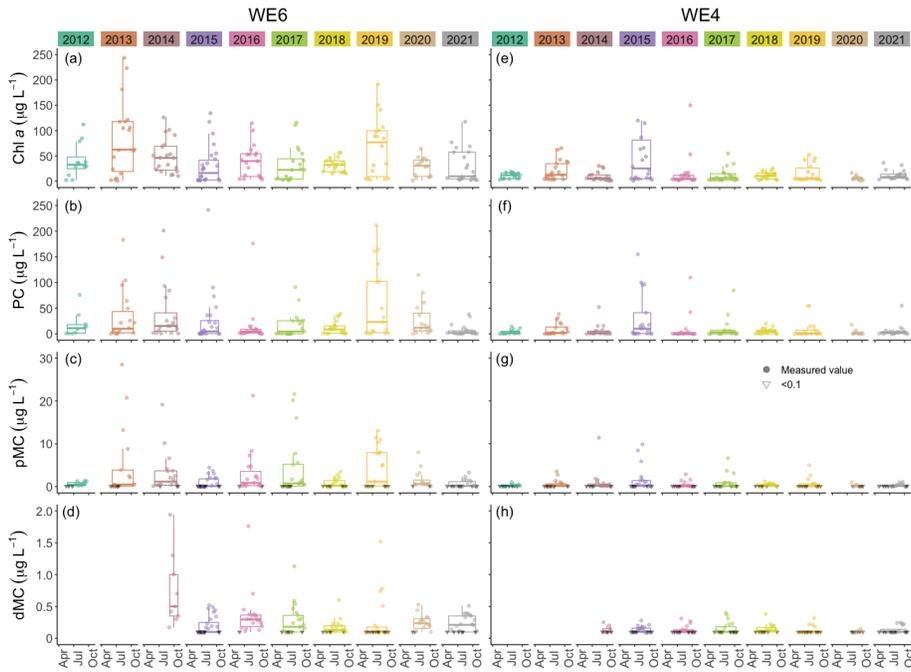
326 Dissolved and particulate microcystins were quantified using a procedure adapted from
327 Wilson et al. (2008). Dissolved microcystins (dMC) were determined through duplicate samples
328 of ~ 2 mL filtrate that was passed through a 0.2 µm membrane filter and stored in glass vials at -
329 20 °C until analysis. Particulate microcystins (pMC) were collected by filtering a known volume
330 of lake water onto a Whatman GF/F glass fiber filter (2012 to 2015) or a 3 µm pore size

332 polycarbonate membrane filter (2016 to 2021). Particulate MC was then extracted from the
333 filters. In sampling years 2012 to 2015, glass fiber filters were submerged in a glass vial
334 containing a 75:25 methanol:water solution (MeOH/H₂O) and sonicated in an ice bath for 2 min.
335 The samples were centrifuged for 15 min and the supernatant was transferred to a clean glass
336 vial. An additional 5 mL of MeOH/H₂O was added to the filter/precipitate and the sample was
337 incubated at -20 °C for 5 h. The sample was then sonicated for 2 min, centrifuged, and the
338 supernatant was removed and added to the first extract vial. The composite supernatant was
339 then centrifuged under a vacuum until dry. The dried extract was then stored at -20 °C until
340 analysis. Particulate MC concentrations were then determined by adding 1 mL of MilliQ water to
341 the sample and using sonication to dissolve the dried extract. For sampling years 2016 to 2021,
342 filters were stored in 2 mL sterile microcentrifuge tubes at -20 °C until analysis. During analysis,
343 pMC were extracted from the membrane filters by adding 1 mL of MilliQ water and subjecting
344 samples to three freeze/thaw cycles at -20 °C followed by addition of Abraxis QuickLyse
345 reagents according to the manufacturer (Eurofins/Abraxis). Particulate MC samples for all
346 sampling years were analyzed immediately after extraction. For all sampling years, dMC and
347 pMC concentrations were determined using a congener-independent enzyme-linked
348 immunosorbent assay (ELISA) kit designed to detect and quantify microcystins and nodularins
349 using the ADDA moiety (Envirologix brand used from 2012 to 2015; Eurofins/Abraxis
350 microcystins/nodularins (ADDA) (EPA ETV) (EPA method 546), ELISA, 96-test kit used from
351 2016 to 2021). Analytical detection limits for the analyses were taken from the manufacturer's
352 documentation.

353 **Results and Discussion**

354 This dataset demonstrates the temporal and spatial variability in water quality
355 parameters in western Lake Erie from 2012 to 2021. Overall, sites closest to the Maumee River
356 inflow (i.e., WE06 and WE09) had the highest median concentrations of nutrients, sediments,
357 pigments, and microcystins compared to sites further out in the basin (i.e., WE02, WE04, and
358 WE13; Table 3). Stations WE06 and WE04 were sampled since the initiation of the monitoring
359 program and consistently represented the high and low extremes of water quality observations
360 during a given time point, respectively, (Table 3) and select parameters for these two sites are
361 represented in figs. 3 and 4. Supplemental figs. 1-16 display the same parameters as figs. 3 and
362 4 for the remaining stations.
363

Deleted: r



365

366 Fig 3. Comparison of chlorophyll a (Chl a), phycocyanin (PC), particulate microcystins (pMC),

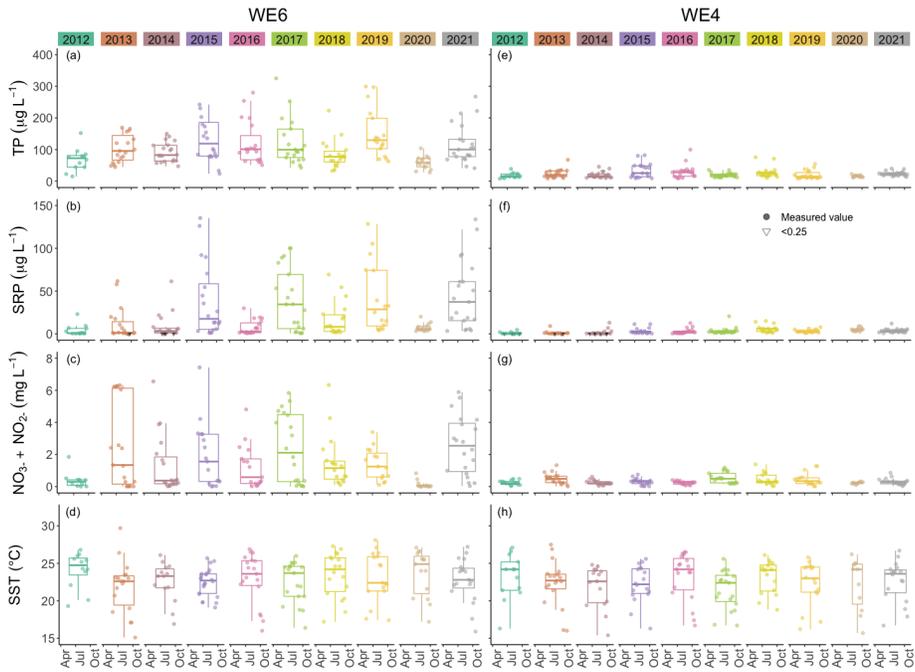
367 and dissolved microcystins (dMC) between stations WE04 and WE06 from 2012 to 2021.

368 Boxplots represent the median and 25% and 75% quartiles with whiskers extending to the

369 highest or lowest point within 1.5x the interquartile range. A scatterplot is overlaid on the

370 boxplots.

371



372

373 Fig 4. Comparison of total phosphorus (TP), soluble reactive phosphorus (SRP), nitrate plus
 374 nitrite ($\text{NO}_3^- + \text{NO}_2^-$), and sea surface temperature (SST) between stations WE04 and WE06
 375 from 2012 to 2021. Boxplots represent the median and 25% and 75% quartiles with whiskers
 376 extending to the highest or lowest point within 1.5x the interquartile range. A scatterplot is
 377 overlaid on the boxplots.

378

379 Table 3. Median values of each parameter at each monitoring station for all surface samples
 380 collected between 2012 to 2021.

Secchi depth (m)	Temp. (°C)	Cond. (µS cm)	DO (mg L ⁻¹)	PAR (µE m ⁻² s ⁻¹)	Beam Attenuation (m ⁻¹)	Transmission (%)	Turbidity (NTU)	Particulate Matter (µg L ⁻¹)	Dissolved Matter (µg L ⁻¹)	Phyco-cyanin (µg L ⁻¹)	Chl-a (µg L ⁻¹)	TP (µg L ⁻¹)	TDP (µg L ⁻¹)	SPP (µg L ⁻¹)	Ammonia (µg L ⁻¹)	Nitrate + Nitrite (mg L ⁻¹)	POC (mg L ⁻¹)	PON (mg L ⁻¹)	CDOM (m ⁻¹)
WE02 0.8	23.1	287	7.7	264	5.1	28.2	9.9	0.78	0.20	4.8	17.5	53.3	12.8	5.7	12.6	0.44	1.4	0.23	0.99
WE04 2.0	22.9	244	7.6	377	2.2	58.4	3.0	0.46	0.17	1.2	7.7	19.2	4.5	2.2	12.9	0.27	0.63	0.10	0.34
WE06 0.5	23.0	346	7.6	173	6.4	20.5	14.8	1.5	0.28	8.0	33.0	90.1	18.7	8.7	11.8	0.83	2.4	0.38	2.0
WE08 1.0	23.3	299	7.7	166	4.3	34.4	9.0	0.88	0.22	5.7	19.5	50.9	12.3	5.8	13.8	0.45	1.5	0.25	1.1
WE09 0.3	23.9	395	7.1	127	12.6	4.3	23.2	0.95	0.26	5.2	32.6	133	44.8	29.5	43.1	1.4	2.5	0.42	2.4
WE12 0.8	23.1	276	7.7	266	5.4	25.9	11.0	0.67	0.16	2.9	15.1	47.6	10.1	5.4	8.4	0.31	1.2	0.20	0.81
WE13 1.5	22.9	244	7.8	456	2.7	52.4	4.3	0.56	0.15	2.6	8.6	22.3	5.0	2.7	10.2	0.25	0.78	0.14	0.38
WE14 1.4	23.2	238	8.1	796	3.7	40.2	7.2	0.80	0.16	17.0	40.0	31.0	4.7	1.5	2.9	0.17	1.7	0.27	0.60
WE15 1.0	23.0	261	7.7	391	3.4	43.0	6.3	0.86	0.19	2.7	12.7	34.8	5.5	2.0	23.9	0.27	1.1	0.18	0.54
WE16 1.3	24.1	269	7.4	297	3.6	40.8	6.3	0.91	0.18	3.4	12.3	30.2	7.2	4.0	10.6	0.30	1.0	0.16	0.71

382 Physicochemical properties

383 Median surface temperatures for all samples across all years ranged from 22.9 to 24.1
384 °C and median benthic temperatures ranged from 22.8 to 23.2 °C (Table 3, Fig. 4), indicating
385 that WLE was thermally well mixed throughout the sampling period. A summary of the dataset
386 indicates that 23.8% of surface temperatures were ≥ 25 °C, and these higher temperatures all
387 occurred from mid-June through the end of September. Bloom forming cyanobacteria species in
388 Lake Erie, including *Microcystis spp.*, often reach maximum growth rates at warmer
389 temperatures (≥ 25 °C) than eukaryotic phytoplankton (Steffen et al., 2014; Huisman et al.,
390 2018). Despite having warmer temperatures that promote recurring HABs, there was only one
391 recorded instance of hypoxia ($\text{DO} < 2 \text{ mg L}^{-1}$) in the dataset and it occurred at WE13 on 08 July
392 2019. Median DO was 7.62 mg L^{-1} in all surface samples and 7.02 mg L^{-1} in all benthic samples
393 from 2012 to 2021 (Table 3), again indicating minimal stratification in WLE during sampling.
394 Median conductivity from 2012 to 2021 was highest at sites WE06 and WE09, which are closest
395 to the Maumee River input, and lowest at sites WE04 and WE13 near the middle of the basin
396 (Table 3). WE06 and WE09 were the only sites to have median conductivity values above 300
397 $\mu\text{S cm}^{-1}$.

398 Optical properties

399 Biotic and abiotic particulate concentrations and movement patterns in WLE are prone to
400 spatial and seasonal variations and are heavily influenced by loading from the Maumee River
401 (Prater et al., 2017; Maguire et al., 2022). Secchi depth, turbidity, and PAR measurements have
402 been correlated with distance from Maumee Bay, where light penetration was lowest near the
403 Maumee River (Chaffin et al., 2011). Variability in optical property measurements in WLE is also
404 dependent on Maumee River inputs, and changes in optical properties can potentially be used

405 in remote sensing algorithms to detect changes in water quality (Sayers et al., 2019). Median
406 Secchi disk depth over the entire dataset was highest at WE04 and lowest at WE06 and WE09,
407 which are closest to the Maumee River (Table 3). Other optical properties, such as PAR, beam
408 attenuation, and transmittance also followed this spatial pattern. In a summary of all samples,
409 median PAR measured at 0.5 m below surface was highest at WE13 and WE14 and lowest at
410 WE09; median transmittance was highest at WE04 and lowest at WE09; and median beam
411 attenuation and turbidity were highest at WE09 and lowest at WE04 (Table 3). Median turbidity
412 values at each site over the 2012 to 2021 period were within the range of previously reported
413 values in the WLE basin (Barbiero and Tuchman, 2004). Median CDOM absorbance and DOC,
414 TSS, and VSS concentrations were again highest at WE09 and lowest at WE04 (Table 3).
415 CDOM gradients in WLE are likewise affected by loading from the Maumee River (Cory et al.,
416 2016) and DOC and CDOM values from this dataset have been used as predictor variables in
417 models estimating PAR attenuation variation in WLE (Weiskerger et al., 2018).

418 Nutrient fractions

419 The Maumee River is a major contributor of nutrients to Lake Erie (Steffen et al., 2014;
420 Kast et al., 2021). Median TP concentrations in WLE from 2012 to 2021 were lowest at WE04
421 and highest at WE09 (Table 3, Fig. 4). Median concentrations at each station from 2012 to 2021
422 were above the GLWQA Annex 4 goals for TP concentration in open waters, which is $15 \mu\text{g P L}^{-1}$
423 for WLE. This goal was met in 92 of 1275 (7.2%) samples and these target values were
424 primarily recorded from stations WE04 and WE13. Sites closer to the mouth of the Maumee
425 River had higher median TP values. While TP loading from the Maumee River tributary declined
426 between 1982 to 2018 (Rowland et al., 2020) the proportion of dissolved P has increased
427 (Joosse and Baker, 2011; Stow et al., 2015). Median TDP values in the WLE dataset were
428 lowest at WE04 and highest at WE09 (Table 3) with a highest recorded value of $274 \mu\text{g P L}^{-1}$ at

429 WE08 in 2015. Median SRP concentrations for each station in this dataset were lowest at WE14
430 and WE15 and were highest at WE09 (Table 3). The maximum recorded SRP concentration
431 was 135.4 $\mu\text{g P L}^{-1}$ at WE06 in 2015 (Fig. 4). Using this dataset, Newell et al. (2019) found that
432 the Maumee River N loading has become more chemically reduced over time where ammonium
433 and PON have increased. Median ammonium concentrations in WLE from 2012 to 2019 were
434 lowest at WE12 and WE14 and highest at WE09 (Table 3) with a recorded maximum
435 concentration of 2109 $\mu\text{g N L}^{-1}$ at WE12 in 2017. Median nitrate + nitrite was lowest at WE13
436 and WE14 and highest at WE09 (Table 3), with a maximum recorded value of 9.5 mg N L^{-1} at
437 WE09 in 2016. See Fig. 4 for a comparison of nitrate + nitrite concentrations between WE04
438 and WE06. Median PON concentrations were lowest at WE04 and highest at WE09 (Table 3)
439 with a recorded max of 40.93 mg N L^{-1} at WE08 in 2015.

Deleted: ammonia

440 Photopigments and microcystins

Deleted: P

441 Median extracted chlorophyll *a* concentrations in surface waters from 2012 to 2021 were
442 lowest at WE04 and highest at WE06 (Table 3, Fig. 3). The highest recorded surface
443 concentration of chlorophyll *a* was 6784 $\mu\text{g L}^{-1}$ on 10 August 2015 at WE08 during the most
444 severe bloom year in this dataset, according to the CI Index (Wynne et al., 2013; Lunetta et al.,
445 2015). The highest measured levels of particulate phycocyanin, pMC, and TP were also
446 recorded at WE06 on 10 August 2015. Other notably high chlorophyll *a* concentrations were
447 measured during severe bloom years in 2017 (532 $\mu\text{g L}^{-1}$ at WE09 on 04 August) and 2019 (593
448 $\mu\text{g L}^{-1}$ at WE09 on 05 August). Similarly, median surface particulate phycocyanin concentration
449 for 2012 to 2021 was highest at WE06 and lowest at WE04 (Table 3, Fig. 4). The highest
450 recorded phycocyanin value was from WE08 on 10 August 2015 (8228 $\mu\text{g L}^{-1}$), followed by 3315
451 $\mu\text{g L}^{-1}$ at WE06 in 2013 during another severe bloom year.

454 Particulate MC concentrations had highest median concentrations at WE06 and were
455 lowest at WE04 (Table 3, Fig. 4), similar to particulate chlorophyll *a* and phycocyanin
456 observations. The highest recorded particulate MC concentration in this dataset was from 10
457 August 2015 at WE08 during a severe bloom year ($297 \mu\text{g L}^{-1}$), followed by $289 \mu\text{g L}^{-1}$ at WE06
458 in 2017 during another severe bloom year according to the CI Index (Wynne et al., 2013;
459 Lunetta et al., 2015). Median dMC concentrations were highest at WE06 and lowest at WE13
460 (Table 3). The maximum dissolved MC in the dataset was $8.19 \mu\text{g L}^{-1}$ at WE09 on 05 August
461 2019, which correlates with high chlorophyll *a* concentrations.

462 Although the United States does not federally enforce water quality criteria or regulations
463 for cyanotoxins in drinking water, the US EPA has a recommended health advisory of $1.6 \mu\text{g L}^{-1}$
464 microcystins in drinking water for school-age children through adults (US EPA, 2015) while the
465 WHO and the Ohio EPA use $1 \mu\text{g L}^{-1}$ microcystins as a guideline (WHO, 2020). From 2012 to
466 2021, 44.4% of pMC samples in this dataset exceeded the WHO guidelines and 34.1%
467 exceeded the US EPA health advisory. Monitoring MC concentrations in western Lake Erie has
468 become especially pertinent since August 2014 when the Toledo, OH drinking water treatment
469 plant was contaminated with microcystins in excess of $1 \mu\text{g L}^{-1}$ and customers were alerted to
470 not drink their tap water until toxin levels were decreased (Steffen et al., 2017). The pMC
471 concentrations at our WLE monitoring stations varied from 1.2-10.1 $\mu\text{g L}^{-1}$ on 04 August 2014
472 during this crisis.

473

474 Data Availability

475 The entire dataset detailed in this manuscript can be freely accessed through the NOAA
476 National Centers for Environmental Information (NCEI) data repository at
477 <https://www.ncei.noaa.gov/>. The data collection is titled "Physical, chemical, and biological water
478 quality monitoring data to support detection of Harmful Algal Blooms (HABs) in western Lake
479 Erie, collected by the Great Lakes Environmental Research Laboratory and the Cooperative
480 Institute for Great Lakes Research since 2012". The digital object identifier is
481 <https://doi.org/10.25921/11da-3x54>. The data presented in this manuscript are available in three
482 separate accession files within this collection including: 2012 to 2018 data is available under
483 NCEI Accession 0187718 v2.2 at <https://www.ncei.noaa.gov/archive/accession/0187718>; 2019
484 data is available under NCEI Accession 0209116 v1.1 at
485 <https://www.ncei.noaa.gov/archive/accession/0209116>; 2020 to 2021 data is available under
486 NCEI Accession 0254720 v1.1 at <https://www.ncei.noaa.gov/archive/accession/0254720>
487 (Cooperative Institute for Great Lakes Research, University of Michigan; NOAA Great Lakes
488 Environmental Research Laboratory, 2019). Future data will be added to this collection as it
489 becomes available.

490 **Conclusions**

491 The western Lake Erie data collected and compiled by NOAA GLERL and CIGLR
492 represent ten years of routine water quality monitoring to detect, track, and predict
493 cyanobacterial HAB events in an area of the Great Lakes that has experienced significant
494 environmental degradation. While this monitoring initiative started in conjunction with remote
495 sensing efforts, it eventually became a standalone program. This ongoing program provides a
496 service to the region and contributes data for investigating the nuanced dynamics of potentially
497 toxic HABs fueled by excess nutrient loading into the WLE basin. For instance, this dataset has
498 assisted in assessing progress toward binational nutrient loading reduction efforts on lake basin
499 concentrations of phosphorus. Long-term monitoring programs like this one provide consistent
500 data which is useful for identifying patterns and variations within the ecosystem and in
501 determining the root cause of those changes. As the sites and parameters of this monitoring
502 program have already changed to adapt to the needs of research, this program will continue to
503 evolve as we consider adding parameters that encompass other aspects of bloom dynamics.
504 For example, lake samples can be analyzed for genomic data that will provide insights on the
505 ability of the current phytoplankton community to produce microcystins. This decadal history has
506 already been an invaluable resource for the research community, and it will continue to enrich
507 our collective scientific knowledge of water quality dynamics in western Lake Erie.

508

509 **Acknowledgements**

510 Funding was awarded to the Cooperative Institute for Great Lakes Research (CIGLR) through
511 the NOAA Cooperative Agreement with the University of Michigan (NA17OAR4320152 and
512 NA22OAR4320150). This is CIGLR contribution number #### and NOAA-GLERL contribution
513 ####. The GLERL/CIGLR monitoring program was supported by the Great Lakes Restoration
514 Initiative. We thank Gabrielle Farina for preparing Fig. 1.

515

516

517 Author Contributions

518 Anna G Boegehold prepared the manuscript. Ashley M. Burtner performed field sampling,
519 laboratory processing, data processing, QA/QC and data management, manuscript revision,
520 data curation. Andrew Camilleri performed field sampling, laboratory processing, manuscript
521 revision. Glenn Carter performed field sampling, laboratory processing, data processing,
522 methodology. Paul DenUyl performed field sampling, laboratory processing, manuscript
523 revision. David Fanslow performed field sampling, laboratory processing. Deanna Fyffe
524 Semenyuk performed field sampling, laboratory processing, manuscript revision. Casey Godwin
525 was responsible for project administration, supervision, visualization, manuscript revision,
526 methodology, field sampling, sample processing. Duane Gossiaux performed field sampling,
527 laboratory processing, manuscript revision, methodology. Tom Johengen was responsible for
528 project administration, supervision, field sampling, methodology. Holly Kelchner performed field
529 sampling, laboratory processing, manuscript revision. Christine Kitchens performed field
530 sampling, laboratory processing, data processing, manuscript revision. Lacey A. Mason was
531 responsible for data curation, manuscript revision. Kelly McCabe performed field sampling,
532 laboratory processing, manuscript revision, methodology. Danna Palladino performed field
533 sampling, laboratory processing, data processing, manuscript revision. Dack Stuart performed
534 field sampling, data processing. Henry Vanderploeg was responsible for project administration,
535 supervision. Reagan Errera was responsible for project administration, supervision,
536 Visualization, manuscript revision, methodology.
537

538 **Competing Interests**

539 The authors declare that they have no conflict of interest

540 References

- 541 Allinger, L. E. and Reavie, E. D.: The ecological history of Lake Erie as recorded by the
542 phytoplankton community, *J. Gt. Lakes Res.*, 39, 365–382,
543 <https://doi.org/10.1016/j.jglr.2013.06.014>, 2013.
- 544 Avouris, D. M. and Ortiz, J. D.: Validation of 2015 Lake Erie MODIS image spectral
545 decomposition using visible derivative spectroscopy and field campaign data, *J. Gt. Lakes Res.*,
546 45, 466–479, <https://doi.org/10.1016/j.jglr.2019.02.005>, 2019.
- 547 Baker, D. B., Ewing, D. E., Johnson, L. T., Kramer, J. W., Merryfield, B. J., Confesor, R. B.,
548 Peter Richards, R., and Roerdink, A. A.: Lagrangian analysis of the transport and processing of
549 agricultural runoff in the lower Maumee River and Maumee Bay, *J. Gt. Lakes Res.*, 40, 479–
550 495, <https://doi.org/10.1016/j.jglr.2014.06.001>, 2014a.
- 551 Baker, D. B., Confesor, R., Ewing, D. E., Johnson, L. T., Kramer, J. W., and Merryfield, B. J.:
552 Phosphorus loading to Lake Erie from the Maumee, Sandusky and Cuyahoga rivers: The
553 importance of bioavailability, *J. Gt. Lakes Res.*, 40, 502–517,
554 <https://doi.org/10.1016/j.jglr.2014.05.001>, 2014b.
- 555 Barbiero, R. P. and Tuchman, M. L.: Long-term Dreissenid Impacts on Water Clarity in Lake
556 Erie, *J. Gt. Lakes Res.*, 30, 557–565, [https://doi.org/10.1016/S0380-1330\(04\)70371-8](https://doi.org/10.1016/S0380-1330(04)70371-8), 2004.
- 557 Berry, M. A., Davis, T. W., Cory, R. M., Duhaime, M. B., Johengen, T. H., Kling, G. W., Marino,
558 J. A., Den Uyl, P. A., Gossiaux, D., Dick, G. J., and Deneff, V. J.: Cyanobacterial harmful algal
559 blooms are a biological disturbance to Western Lake Erie bacterial communities, *Environ.*
560 *Microbiol.*, 19, 1149–1162, <https://doi.org/10.1111/1462-2920.13640>, 2017.
- 561 Bertani, I., Steger, C. E., Obenour, D. R., Fahnenstiel, G. L., Bridgeman, T. B., Johengen, T. H.,
562 Sayers, M. J., Shuchman, R. A., and Scavia, D.: Tracking cyanobacteria blooms: Do different
563 monitoring approaches tell the same story?, *Sci. Total Environ.*, 575, 294–308,
564 <https://doi.org/10.1016/j.scitotenv.2016.10.023>, 2017.
- 565 Binding, C. E., Jerome, J. H., Bukata, R. P., and Booty, W. G.: Spectral absorption properties of
566 dissolved and particulate matter in Lake Erie, *Remote Sens. Environ.*, 112, 1702–1711,
567 <https://doi.org/10.1016/j.rse.2007.08.017>, 2008.
- 568 Bosse, K. R., Sayers, M. J., Shuchman, R. A., Fahnenstiel, G. L., Ruberg, S. A., Fanslow, D. L.,
569 Stuart, D. G., Johengen, T. H., and Burtner, A. M.: Spatial-temporal variability of in situ
570 cyanobacteria vertical structure in Western Lake Erie: Implications for remote sensing
571 observations, *J. Gt. Lakes Res.*, 45, 480–489, <https://doi.org/10.1016/j.jglr.2019.02.003>, 2019.
- 572 Bridoux, M., Sobiechowska, M., Perez-Fuentetaja, A., and Alben, K. T.: Algal pigments in Lake
573 Erie dreissenids, pseudofeces and sediments, as tracers of diet, selective feeding and
574 bioaccumulation, *J. Gt. Lakes Res.*, 36, 437–447, <https://doi.org/10.1016/j.jglr.2010.06.005>,
575 2010.
- 576 Buratti, F. M., Manganelli, M., Vichi, S., Stefanelli, M., Scardala, S., Testai, E., and Funari, E.:
577 Cyanotoxins: producing organisms, occurrence, toxicity, mechanism of action and human health

578 toxicological risk evaluation, *Arch. Toxicol.*, 91, 1049–1130, [https://doi.org/10.1007/s00204-016-](https://doi.org/10.1007/s00204-016-1913-6)
579 1913-6, 2017.

580 Carmichael, W. W. and Boyer, G. L.: Health impacts from cyanobacteria harmful algae blooms:
581 Implications for the North American Great Lakes, *Harmful Algae*, 54, 194–212,
582 <https://doi.org/10.1016/j.hal.2016.02.002>, 2016.

583 Chaffin, J. D. and Bridgeman, T. B.: Organic and inorganic nitrogen utilization by nitrogen-
584 stressed cyanobacteria during bloom conditions, *J. Appl. Phycol.*, 26, 299–309,
585 <https://doi.org/10.1007/s10811-013-0118-0>, 2014.

586 Chaffin, J. D., Bridgeman, T. B., Heckathorn, S. A., and Mishra, S.: Assessment of *Microcystis*
587 growth rate potential and nutrient status across a trophic gradient in western Lake Erie, *J. Gt.*
588 *Lakes Res.*, 37, 92–100, <https://doi.org/10.1016/j.jglr.2010.11.016>, 2011.

589 Charlton, M. N., Milne, J. E., Booth, W. G., and Chiochio, F.: Lake Erie Offshore in 1990:
590 Restoration and Resilience in the Central Basin, *J. Gt. Lakes Res.*, 19, 291–309,
591 [https://doi.org/10.1016/S0380-1330\(93\)71218-6](https://doi.org/10.1016/S0380-1330(93)71218-6), 1993.

592 Conroy, J. D., Kane, D. D., Dolan, D. M., Edwards, W. J., Charlton, M. N., and Culver, D. A.:
593 Temporal Trends in Lake Erie Plankton Biomass: Roles of External Phosphorus Loading and
594 Dreissenid Mussels, *J. Gt. Lakes Res.*, 31, 89–110, [https://doi.org/10.1016/S0380-](https://doi.org/10.1016/S0380-1330(05)70307-5)
595 1330(05)70307-5, 2005.

596 Cooperative Institute for Great Lakes Research, University of Michigan; NOAA Great Lakes
597 Environmental Research Laboratory: Physical, chemical, and biological water quality monitoring
598 data to support detection of Harmful Algal Blooms (HABs) in western Lake Erie, collected by the
599 Great Lakes Environmental Research Laboratory and the Cooperative Institute for Great Lakes
600 Research since 2012, NOAA National Centers for Environmental Information [data set],
601 <https://doi.org/10.25921/11da-3x54>, 2019.

602 Cory, R. M., Davis, T. W., Dick, G. J., Johengen, T., Deneff, V. J., Berry, M. A., Page, S. E.,
603 Watson, S. B., Yuhas, K., and Kling, G. W.: Seasonal Dynamics in Dissolved Organic Matter,
604 Hydrogen Peroxide, and Cyanobacterial Blooms in Lake Erie, *Front. Mar. Sci.*, 3, 2016.

605 Cousino, L. K., Becker, R. H., and Zmijewski, K. A.: Modeling the effects of climate change on
606 water, sediment, and nutrient yields from the Maumee River watershed, *J. Hydrol. Reg. Stud.*, 4,
607 762–775, <https://doi.org/10.1016/j.ejrh.2015.06.017>, 2015.

608 Den Uyl, P. A., Harrison, S. B., Godwin, C. M., Rowe, M. D., Strickler, J. R., and Vanderploeg,
609 H. A.: Comparative analysis of *Microcystis* buoyancy in western Lake Erie and Saginaw Bay of
610 Lake Huron, *Harmful Algae*, 108, 102102, <https://doi.org/10.1016/j.hal.2021.102102>, 2021.

611 Den Uyl, P. A., Thompson, L. R., Errera, R. M., Birch, J. M., Preston, C. M., Ussler, W. I.,
612 Yancey, C. E., Chaganti, S. R., Ruberg, S. A., Doucette, G. J., Dick, G. J., Scholin, C. A., and
613 Goodwin, K. D.: Lake Erie field trials to advance autonomous monitoring of cyanobacterial
614 harmful algal blooms, *Front. Mar. Sci.*, 9, <https://doi.org/10.3389/fmars.2022.1021952>, 2022.

615 Dolan, D. M. and Chapra, S. C.: Great Lakes total phosphorus revisited: 1. Loading analysis
616 and update (1994–2008), *J. Gt. Lakes Res.*, 38, 730–740,
617 <https://doi.org/10.1016/j.jglr.2012.10.001>, 2012.

618 Environment and Climate Change Canada and the U.S. Environmental Protection Agency.
619 2022. State of the Great Lakes 2022 Technical Report. Cat No. En161-3/1E-PDF. EPA 905-
620 R22-004. Available at binational.net, 2022.

621 Fang, S., Del Giudice, D., Scavia, D., Binding, C. E., Bridgeman, T. B., Chaffin, J. D., Evans, M.
622 A., Guinness, J., Johengen, T. H., and Obenour, D. R.: A space-time geostatistical model for
623 probabilistic estimation of harmful algal bloom biomass and areal extent, *Sci. Total Environ.*,
624 695, 133776, <https://doi.org/10.1016/j.scitotenv.2019.133776>, 2019.

625 Goeyens, L., Kindermans, N., Abu Yusuf, M., and Elskens, M.: A Room Temperature Procedure
626 for the Manual Determination of Urea in Seawater, *Estuar. Coast. Shelf Sci.*, 47, 415–418,
627 <https://doi.org/10.1006/ecss.1998.0357>, 1998.

628 Hartig, J. H., Zarull, M. A., Ciborowski, J. J. H., Gannon, J. E., Wilke, E., Norwood, G., and
629 Vincent, A. N.: Long-term ecosystem monitoring and assessment of the Detroit River and
630 Western Lake Erie, *Environ. Monit. Assess.*, 158, 87–104, <https://doi.org/10.1007/s10661-008-0567-0>, 2009.

632 GLWQA: Great Lakes Water Quality Agreement; Protocol Amending the Agreement Between
633 Canada and the United States of America on Great Lakes Water Quality, 1978, as Amended on
634 October 16, 1983 and on November 18, 1987, <https://binational.net/2012/09/05/2012-glwqa-aeqgl/> (last access: November 2022), 2012.

636
637 Hartig, J. H., Francoeur, S. N., Ciborowski, J. J. H., Gannon, J. E., Sanders, C. E., Galvao-
638 Ferreira, P., Knauss, C. R., Gell, G., and Berk, K.: An ecosystem health assessment of the
639 Detroit River and western Lake Erie, *J. Gt. Lakes Res.*, 47, 1241–1256,
640 <https://doi.org/10.1016/j.jglr.2021.05.008>, 2021.

641 Hedges, J. I. and Stern, J. H.: Carbon and nitrogen determinations of carbonate-containing
642 solids¹, *Limnol. Oceanogr.*, 29, 657–663, <https://doi.org/10.4319/lo.1984.29.3.0657>, 1984.

643 Hellweger, F. L., Martin, R. M., Eigemann, F., Smith, D. J., Dick, G. J., and Wilhelm, S. W.:
644 Models predict planned phosphorus load reduction will make Lake Erie more toxic, *Science*,
645 376, 1001–1005, <https://doi.org/10.1126/science.abm6791>, 2022.

646 Hoffman, D. K., McCarthy, M. J., Boedecker, A. R., Myers, J. A., and Newell, S. E.: The role of
647 internal nitrogen loading in supporting non-N-fixing harmful cyanobacterial blooms in the water
648 column of a large eutrophic lake, *Limnol. Oceanogr.*, n/a, <https://doi.org/10.1002/lno.12185>,
649 2022.

650 Horváth, H., Kovács, A. W., Riddick, C., and Présing, M.: Extraction methods for phycocyanin
651 determination in freshwater filamentous cyanobacteria and their application in a shallow lake,
652 *Eur. J. Phycol.*, 48, 278–286, <https://doi.org/10.1080/09670262.2013.821525>, 2013.

653 Huisman, J., Codd, G. A., Paerl, H. W., Ibelings, B. W., Verspagen, J. M. H., and Visser, P. M.:
654 Cyanobacterial blooms | *Nature Reviews Microbiology*, *Nat. Rev. Microbiol.*, 16, 471–483,
655 <https://doi.org/10.1038/s41579-018-0040-1>, 2018.

656 Joosse, P. J. and Baker, D. B.: Context for re-evaluating agricultural source phosphorus
657 loadings to the Great Lakes, *Can. J. Soil Sci.*, 91, 317–327, <https://doi.org/10.4141/cjss10005>,
658 2011.

659 Kane, D. D., Ludsin, S. A., Briland, R. D., Culver, D. A., and Munawar, M.: Ten+years gone:
660 Continued degradation of offshore planktonic communities in U.S. waters of Lake Erie's western
661 and central basins (2003–2013), *J. Gt. Lakes Res.*, 41, 930–933,
662 <https://doi.org/10.1016/j.jglr.2015.06.002>, 2015.

663 Kast, J. B., Apostel, A. M., Kalcic, M. M., Muenich, R. L., Dagnew, A., Long, C. M., Evenson, G.,
664 and Martin, J. F.: Source contribution to phosphorus loads from the Maumee River watershed to
665 Lake Erie, *J. Environ. Manage.*, 279, 111803, <https://doi.org/10.1016/j.jenvman.2020.111803>,
666 2021.

667 Kharbush, J. J., Smith, D. J., Powers, M., Vanderploeg, H. A., Fanslow, D., Robinson, R. S.,
668 Dick, G. J., and Pearson, A.: Chlorophyll nitrogen isotope values track shifts between
669 cyanobacteria and eukaryotic algae in a natural phytoplankton community in Lake Erie, *Org.*
670 *Geochem.*, 128, 71–77, <https://doi.org/10.1016/j.orggeochem.2018.12.006>, 2019.

671 Kharbush, J. J., Robinson, R. S., and Carter, S. J.: Patterns in sources and forms of nitrogen in
672 a large eutrophic lake during a cyanobacterial harmful algal bloom, *Limnol. Oceanogr.*, n/a,
673 <https://doi.org/10.1002/lno.12311>, 2023.

674 King, W. M., Curless, S. E., and Hood, J. M.: River phosphorus cycling during high flow may
675 constrain Lake Erie cyanobacteria blooms, *Water Res.*, 222, 118845,
676 <https://doi.org/10.1016/j.watres.2022.118845>, 2022.

677 Liu, Q., Rowe, M. D., Anderson, E. J., Stow, C. A., Stumpf, R. P., and Johengen, T. H.:
678 Probabilistic forecast of microcystin toxin using satellite remote sensing, in situ observations and
679 numerical modeling, *Environ. Model. Softw.*, 128, 104705,
680 <https://doi.org/10.1016/j.envsoft.2020.104705>, 2020.

681 Lunetta, R. S., Schaeffer, B. A., Stumpf, R. P., Keith, D., Jacobs, S. A., and Murphy, M. S.:
682 Evaluation of cyanobacteria cell count detection derived from MERIS imagery across the
683 eastern USA, *Remote Sens. Environ.*, 157, 24–34, <https://doi.org/10.1016/j.rse.2014.06.008>,
684 2015.

685 Maguire, T. J., Stow, C. A., and Godwin, C. M.: Spatially referenced Bayesian state-space
686 model of total phosphorus in western Lake Erie, *Hydrol. Earth Syst. Sci.*, 26, 1993–2017,
687 <https://doi.org/10.5194/hess-26-1993-2022>, 2022.

688 Makarewicz, J. C. and Bertram, P.: Evidence for the Restoration of the Lake Erie Ecosystem:
689 Water quality, oxygen levels, and pelagic function appear to be improving, *BioScience*, 41, 216–
690 223, <https://doi.org/10.2307/1311411>, 1991.

691 Marino, J. A., Deneff, V. J., Dick, G. J., Duhaime, M. B., and James, T. Y.: Fungal community
692 dynamics associated with harmful cyanobacterial blooms in two Great Lakes, *J. Gt. Lakes Res.*,
693 48, 1021–1031, <https://doi.org/10.1016/j.jglr.2022.05.007>, 2022.

694 Matisoff, G., Kaltenberg, E. M., Steely, R. L., Hummel, S. K., Seo, J., Gibbons, K. J.,
695 Bridgeman, T. B., Seo, Y., Behbahani, M., James, W. F., Johnson, L. T., Doan, P., Dittrich, M.,
696 Evans, M. A., and Chaffin, J. D.: Internal loading of phosphorus in western Lake Erie, *J. Gt.*
697 *Lakes Res.*, 42, 775–788, <https://doi.org/10.1016/j.jglr.2016.04.004>, 2016.

698 Michalak, A. M., Anderson, E. J., Beletsky, D., Boland, S., Bosch, N. S., Bridgeman, T. B.,
699 Chaffin, J. D., Cho, K., Confesor, R., Daloğlu, I., DePinto, J. V., Evans, M. A., Fahnenstiel, G. L.,
700 He, L., Ho, J. C., Jenkins, L., Johengen, T. H., Kuo, K. C., LaPorte, E., Liu, X., McWilliams, M.
701 R., Moore, M. R., Posselt, D. J., Richards, R. P., Scavia, D., Steiner, A. L., Verhamme, E.,
702 Wright, D. M., and Zagorski, M. A.: Record-setting algal bloom in Lake Erie caused by
703 agricultural and meteorological trends consistent with expected future conditions, *Proc. Natl.*
704 *Acad. Sci.*, 110, 6448–6452, <https://doi.org/10.1073/pnas.1216006110>, 2013.

705 Mitchell, B.G., Kahru, M., Wieland, J., and Stramska, M.: Determination of spectral absorption
706 coefficients of particles, dissolved material and phytoplankton for discrete water samples, In:
707 Mueller, J.L., G.S. Fargion, and C.R. McClain [Eds.] *Ocean Optics Protocols for Satellite Ocean*
708 *Color Sensor Validation, Revision 4, Volume IV: Inherent Optical Properties: Instruments,*
709 *Characterizations, Field Measurements and Data Analysis Protocols. NASA/TM- 2003-211621,*
710 *NASA Goddard Space Flight Center, Greenbelt, MD, Chapter 4, pp 39-64, 2003.*

711 Mohamed, M. N., Wellen, C., Parsons, C. T., Taylor, W. D., Arhonditsis, G., Chomicki, K. M.,
712 Boyd, D., Weidman, P., Mundle, S. O. C., Cappellen, P. V., Sharpley, A. N., and Haffner, D. G.:
713 Understanding and managing the re-eutrophication of Lake Erie: Knowledge gaps and research
714 priorities, *Freshw. Sci.*, 38, 675–691, <https://doi.org/10.1086/705915>, 2019.

715 Mulvenna, P. F. and Savidge, G.: A modified manual method for the determination of urea in
716 seawater using diacetylmonoxime reagent, *Estuar. Coast. Shelf Sci.*, 34, 429–438,
717 [https://doi.org/10.1016/S0272-7714\(05\)80115-5](https://doi.org/10.1016/S0272-7714(05)80115-5), 1992.

718 Myers, D.N., Thomas, M.A., Frey, J.W., Rheume, S.J., and Button, D.T.: Water Quality in the
719 Lake Erie-Lake Saint Clair Drainages Michigan, Ohio, Indiana, New York, and Pennsylvania,
720 1996–98: U.S. Geological Survey Circular 1203, 35 p., <https://pubs.water.usgs.gov/circ1203/>,
721 2000.
722

723 [NCWQR: Heidelberg Tributary Loading Program \(HTLP\) Dataset. Zenodo.](https://doi.org/10.5281/zenodo.6606949)
724 <https://doi.org/10.5281/zenodo.6606949>, 2022.

725 Newell, S. E., Davis, T. W., Johengen, T. H., Gossiaux, D., Burtner, A., Palladino, D., and
726 McCarthy, M. J.: Reduced forms of nitrogen are a driver of non-nitrogen-fixing harmful
727 cyanobacterial blooms and toxicity in Lake Erie, *Harmful Algae*, 81, 86–93,
728 <https://doi.org/10.1016/j.hal.2018.11.003>, 2019.

729 Pirasteh, S., Mollae, S., Fatholahi, S. N., and Li, J.: Estimation of Phytoplankton Chlorophyll-a
730 Concentrations in the Western Basin of Lake Erie Using Sentinel-2 and Sentinel-3 Data, *Can. J.*
731 *Remote Sens.*, 46, 585–602, <https://doi.org/10.1080/07038992.2020.1823825>, 2020.

732 Prater, C., Frost, P. C., Howell, E. T., Watson, S. B., Zastepa, A., King, S. S. E., Vogt, R. J., and
733 Xenopoulos, M. A.: Variation in particulate C : N : P stoichiometry across the Lake Erie
734 watershed from tributaries to its outflow, *Limnol. Oceanogr.*, 62, S194–S206,
735 <https://doi.org/10.1002/lno.10628>, 2017.

736 Qian, S. S., Stow, C. A., Rowland, F. E., Liu, Q., Rowe, M. D., Anderson, E. J., Stumpf, R. P.,
737 and Johengen, T. H.: Chlorophyll a as an indicator of microcystin: Short-term forecasting and
738 risk assessment in Lake Erie, *Ecol. Indic.*, 130, 108055,
739 <https://doi.org/10.1016/j.ecolind.2021.108055>, 2021.

- 740 Reavie, E. D., Cai, M., Twiss, M. R., Carrick, H. J., Davis, T. W., Johengen, T. H., Gossiaux, D.,
741 Smith, D. E., Palladino, D., Burtner, A., and Sgro, G. V.: Winter–spring diatom production in
742 Lake Erie is an important driver of summer hypoxia, *J. Gt. Lakes Res.*, 42, 608–618,
743 <https://doi.org/10.1016/j.jglr.2016.02.013>, 2016.
- 744 Rowe, M. D., Anderson, E. J., Wynne, T. T., Stumpf, R. P., Fanslow, D. L., Kijanka, K.,
745 Vanderploeg, H. A., Strickler, J. R., and Davis, T. W.: Vertical distribution of buoyant *Microcystis*
746 blooms in a Lagrangian particle tracking model for short-term forecasts in Lake Erie, *J.*
747 *Geophys. Res. Oceans*, 121, 5296–5314, <https://doi.org/10.1002/2016JC011720>, 2016.
- 748 Rowland, F. E., Stow, C. A., Johengen, T. H., Burtner, A. M., Palladino, D., Gossiaux, D. C.,
749 Davis, T. W., Johnson, L. T., and Ruberg, S.: Recent Patterns in Lake Erie Phosphorus and
750 Chlorophyll *a* Concentrations in Response to Changing Loads, *Environ. Sci. Technol.*, 54, 835–
751 841, <https://doi.org/10.1021/acs.est.9b05326>, 2020.
- 752 Sayers, M., Fahnenstiel, G. L., Shuchman, R. A., and Whitley, M.: Cyanobacteria blooms in
753 three eutrophic basins of the Great Lakes: a comparative analysis using satellite remote
754 sensing, *Int. J. Remote Sens.*, 37, 4148–4171, <https://doi.org/10.1080/01431161.2016.1207265>,
755 2016.
- 756 Sayers, M. J., Bosse, K. R., Shuchman, R. A., Ruberg, S. A., Fahnenstiel, G. L., Leshkevich, G.
757 A., Stuart, D. G., Johengen, T. H., Burtner, A. M., and Palladino, D.: Spatial and temporal
758 variability of inherent and apparent optical properties in western Lake Erie: Implications for
759 water quality remote sensing, *J. Gt. Lakes Res.*, 45, 490–507,
760 <https://doi.org/10.1016/j.jglr.2019.03.011>, 2019.
- 761 Smith, D. J., Tan, J. Y., Powers, M. A., Lin, X. N., Davis, T. W., and Dick, G. J.: Individual
762 *Microcystis* colonies harbour distinct bacterial communities that differ by *Microcystis* oligotype
763 and with time, *Environ. Microbiol.*, 23, 3020–3036, <https://doi.org/10.1111/1462-2920.15514>,
764 2021.
- 765 Smith, D. J., Berry, M. A., Cory, R. M., Johengen, T. H., Kling, G. W., Davis, T. W., and Dick, G.
766 J.: Heterotrophic Bacteria Dominate Catalase Expression during *Microcystis* Blooms, *Appl.*
767 *Environ. Microbiol.*, 88, e02544-21, <https://doi.org/10.1128/aem.02544-21>, 2022.
- 768 Smith, R. B., Bass, B., Sawyer, D., Depew, D., and Watson, S. B.: Estimating the economic
769 costs of algal blooms in the Canadian Lake Erie Basin, *Harmful Algae*, 87, 101624,
770 <https://doi.org/10.1016/j.hal.2019.101624>, 2019.
- 771 Speziale, B. J., Schreiner, S. P., Giammatteo, P. A., and Schindler, J. E.: Comparison of N,N-
772 Dimethylformamide, Dimethyl Sulfoxide, and Acetone for Extraction of Phytoplankton
773 Chlorophyll, *Can. J. Fish. Aquat. Sci.*, 41, 1519–1522, <https://doi.org/10.1139/f84-187>, 1984.
- 774 Standard Methods Committee of the American Public Health Association, American Water
775 Works Association, and Water Environment Federation: Standard Methods For the Examination
776 of Water and Wastewater, 23rd edition, Sections 2540 Solids, 4500-P Phosphorus, 4500-nh3-
777 nitrogen (ammonia), 4500-no3-nitrogen (nitrate), 5310 Total Organic Carbon, edited by: Lipps
778 WC, Baxter TE, Braun-Howland E, APHA Press, Washington, DC, ISBN 1625762402, 2017.

779 Steffen, M. M., Belisle, B. S., Watson, S. B., Boyer, G. L., and Wilhelm, S. W.: Status, causes
780 and controls of cyanobacterial blooms in Lake Erie, *J. Gt. Lakes Res.*, 40, 215–225,
781 <https://doi.org/10.1016/j.jglr.2013.12.012>, 2014.

782 Steffen, M. M., Davis, T. W., McKay, R. M. L., Bullerjahn, G. S., Krausfeldt, L. E., Stough, J. M.
783 A., Neitzey, M. L., Gilbert, N. E., Boyer, G. L., Johengen, T. H., Gossiaux, D. C., Burtner, A. M.,
784 Palladino, D., Rowe, M. D., Dick, G. J., Meyer, K. A., Levy, S., Boone, B. E., Stumpf, R. P.,
785 Wynne, T. T., Zimba, P. V., Gutierrez, D., and Wilhelm, S. W.: Ecophysiological Examination of
786 the Lake Erie Microcystis Bloom in 2014: Linkages between Biology and the Water Supply
787 Shutdown of Toledo, OH, *Environ. Sci. Technol.*, 51, 6745–6755,
788 <https://doi.org/10.1021/acs.est.7b00856>, 2017.

789 Sterner, R. W., Keeler, B., Polasky, S., Poudel, R., Rhude, K., and Rogers, M.: Ecosystem
790 services of Earth's largest freshwater lakes, *Ecosyst. Serv.*, 41, 101046,
791 <https://doi.org/10.1016/j.ecoser.2019.101046>, 2020.

792 Stow, C. A., Cha, Y., Johnson, L. T., Confesor, R., and Richards, R. P.: Long-Term and
793 Seasonal Trend Decomposition of Maumee River Nutrient Inputs to Western Lake Erie, *Environ.*
794 *Sci. Technol.*, 49, 3392–3400, <https://doi.org/10.1021/es5062648>, 2015.

795 US EPA - United States Environmental Protection Agency: Method 180.1: Determination of
796 Turbidity by Nephelometry, Revision 2.0, Edited by: O'Dell, J.W., 1993.

797 US EPA - United States Environmental Protection Agency: Drinking Water Health Advisory for
798 the Cyanobacterial Microcystin Toxins, EPA Document Number 820R15100, 2015.
799

800 Van Meter, K. J., McLeod, M. M., Liu, J., Tenkouano, G. T., Hall, R. I., Van Cappellen, P., and
801 Basu, N. B.: Beyond the Mass Balance: Watershed Phosphorus Legacies and the Evolution of
802 the Current Water Quality Policy Challenge, *Water Resour. Res.*, 57, e2020WR029316,
803 <https://doi.org/10.1029/2020WR029316>, 2021.

804 Vander Woude, A., Ruberg, S., Johengen, T., Miller, R., and Stuart, D.: Spatial and temporal
805 scales of variability of cyanobacteria harmful algal blooms from NOAA GLERL airborne
806 hyperspectral imagery, *J. Gt. Lakes Res.*, 45, 536–546,
807 <https://doi.org/10.1016/j.jglr.2019.02.006>, 2019.

808 Vanderploeg, H. A., Liebig, J. R., Carmichael, W. W., Agy, M. A., Johengen, T. H., Fahnenstiel,
809 G. L., and Nalepa, T. F.: Zebra mussel (*Dreissena polymorpha*) selective filtration promoted
810 toxic Microcystis blooms in Saginaw Bay (Lake Huron) and Lake Erie, *Can. J. Fish. Aquat. Sci.*,
811 58, 1208–1221, <https://doi.org/10.1139/f01-066>, 2001.

812 Wang, Q. and Boegman, L.: Multi-Year Simulation of Western Lake Erie Hydrodynamics and
813 Biogeochemistry to Evaluate Nutrient Management Scenarios, *Sustainability*, 13, 7516,
814 <https://doi.org/10.3390/su13147516>, 2021.

815 Watson, S. B., Miller, C., Arhonditsis, G., Boyer, G. L., Carmichael, W., Charlton, M. N.,
816 Confesor, R., Depew, D. C., Höök, T. O., Ludsins, S. A., Matisoff, G., McElmurry, S. P., Murray,
817 M. W., Peter Richards, R., Rao, Y. R., Steffen, M. M., and Wilhelm, S. W.: The re-eutrophication
818 of Lake Erie: Harmful algal blooms and hypoxia, *Harmful Algae*, 56, 44–66,
819 <https://doi.org/10.1016/j.hal.2016.04.010>, 2016.

820 Weiskerger, C. J., Rowe, M. D., Stow, C. A., Stuart, D., and Johengen, T.: Application of the
821 Beer–Lambert Model to Attenuation of Photosynthetically Active Radiation in a Shallow,
822 Eutrophic Lake, *Water Resour. Res.*, 54, 8952–8962, <https://doi.org/10.1029/2018WR023024>,
823 2018.

824 Wetzel, R.G., and Likens G.E.: *Limnological Analyses*, 3rd edition, Springer New York, NY,
825 <https://doi.org/10.1007/978-1-4757-3250-4>, 2000.

826 WHO - World Health Organization: Cyanobacterial toxins: microcystins. Background document
827 for development of WHO Guidelines for drinking-water quality and Guidelines for safe
828 recreational water environments, WHO/HEP/ECH/WSH/2020.6, 2020.
829

830 Wilson, A. E., Gossiaux, D. C., Höök, T. O., Berry, J. P., Landrum, P. F., Dyble, J., and
831 Guildford, S. J.: Evaluation of the human health threat associated with the hepatotoxin
832 microcystin in the muscle and liver tissues of yellow perch (*Perca flavescens*), *Can. J. Fish.*
833 *Aquat. Sci.*, 65, 1487–1497, <https://doi.org/10.1139/F08-067>, 2008.

834 Wynne, T. T., Stumpf, R. P., Tomlinson, M. C., Fahnenstiel, G. L., Dyble, J., Schwab, D. J., and
835 Joshi, S. J.: Evolution of a cyanobacterial bloom forecast system in western Lake Erie:
836 Development and initial evaluation, *J. Gt. Lakes Res.*, 39, 90–99,
837 <https://doi.org/10.1016/j.jglr.2012.10.003>, 2013.

838 Xu, J., Liu, H., Lin, J., Lyu, H., Dong, X., Li, Y., Guo, H., and Wang, H.: Long-term monitoring
839 particulate composition change in the Great Lakes using MODIS data, *Water Res.*, 222,
840 118932, <https://doi.org/10.1016/j.watres.2022.118932>, 2022.

841 Yancey, C.E., Mathiesen, O., and Dick, G.J.: Transcriptionally active nitrogen fixation and
842 biosynthesis of diverse secondary metabolites by *Dolichospermum* and *Aphanizominom*-like
843 Cyanobacteria in western Lake Erie *Microcystis* blooms, *bioRxiv* [preprint],
844 <https://doi.org/10.1101/2022.09.30.510322> 01 October 2022a.

845 Yancey, C. E., Smith, D. J., Den Uyl, P. A., Mohamed, O. G., Yu, F., Ruberg, S. A., Chaffin, J.
846 D., Goodwin, K. D., Tripathi, A., Sherman, D. H., and Dick, G. J.: Metagenomic and
847 Metatranscriptomic Insights into Population Diversity of *Microcystis* Blooms: Spatial and
848 Temporal Dynamics of *mcy* Genotypes, Including a Partial Operon That Can Be Abundant and
849 Expressed, *Appl. Environ. Microbiol.*, 88, e02464-21, <https://doi.org/10.1128/aem.02464-21>,
850 2022b.